JOURNAL OF SOLID STATE CHEMISTRY 99, 189–199 (1992)

Importance of Short Interlayer Te···Te Contacts for the Structural Distortions and Physical Properties of CdI_2-Type Layered Transition-Metal Ditellurides

ENRIC CANADELL

Laboratoire de Chimie Théorique, Bât. 490, Université de Paris-Sud, 91405 Orsay, France

STÉPHANE JOBIC, RAYMOND BREC, AND JEAN ROUXEL

Laboratoire de Chimie des Solides, Institut des Matériaux de Nantes, 2 rue de la Houssinière, 44072 Nantes Cédex 03, France

AND MYUNG-HWAN WHANGBO

Department of Chemistry, North Carolina State University, Raleigh, North Carolina 27695-8204

Received October 10, 1991; in revised form January 20, 1992; accepted January 23, 1992

THIS WORK IS DEDICATED TO PROFESSOR NEIL BARTLETT ON THE OCCASION OF HIS 60th BIRTHDAY

We examined how the short intra- and interlayer Te···Te contacts of layered transition-metal tellurides affect their structures and physical properties by carrying out tight-binding band electronic structure calculations for the CdI_2-type layered transition-metal dichalcogenides TiX_2 (X = S, Se, Te) and MTe_2 (M = V, Nb, Ta) on the basis of the extended Hückel method. In the CdI_2-type tellurides, the top portion of the Te p-block bands overlaps significantly with the bottom portion of the metal d-block bands, thereby causing a substantial electron transfer from the p- to the d-block bands. For this $p \rightarrow d$ electron transfer, the interlayer Te···Te contacts are found to be essential because the overlap between the Te p_z-orbitals (perpendicular to the layer) associated with the interlayer Te···Te contacts is most effective in raising the top portion of the Te p-block bands. As a consequence, layered transition-metal tellurides are likely to possess a three-dimensional metallic character, and a slight change in their interlayer Te···Te contacts significantly affects their electrical and other physical properties.

Layered transition-metal tellurides frequently possess intra- and interlayer Te···Te contacts shorter than the van der Waals (VDW) radii sum (i.e., 4.0 Å) (*1*). In the field of organic salts (*2*) based upon sulfur-containing donor molecules, it is well established that intermolecular S···S contacts shorter than, or in the vicinity of, the VDW sum (i.e., 3.6 Å) are found to be crucial for whether the salts are one-dimensional (1D) metals, two-dimensional (2D) metals, or insulators. By analogy, short Te···Te contacts of layered transition-metal tellurides are expected to be important for their structural

0022-4596/92 $5.00

and electronic properties. In fact, short interlayer Se···Se distances in $NbSe_3$ and $TaSe_3$ (*3*), short interlayer Te···Te distances in $ZrTe_3$ (*4*), and short intra- and interlayer Te···Te distances in β-$MoTe_2$ (*5*) are found to be crucial in understanding the dimensionality of the metallic properties of these chalcogenides. The presence of short Te···Te contacts in layered transition-metal tellurides and their importance in controlling the physical properties of these tellurides have been recognized in a number of recent studies (*4–9*). However, there has been no systematic evaluation of how the structures and the physical properties of layered tellurides could be affected by their short Te···Te contacts. In the present work, therefore, we analyze the electronic structures of several CdI_2-type layered transition-metal dichalcogenides MX_2 so as to evaluate the role that short Te···Te contacts play in layered tellurides.

To a first approximation, the oxidation state of a CdI_2-type transition-metal dichalcogenides MX_2 is given by $M^{4+}(X^{2-})_2$. Typically, this implies that the chalcogen *p*-block bands are completely filled, and lie below the metal *d*-block bands. In general, the top portion of the chalcogen *p*-block bands, being antibonding in character between adjacent chalcogen atoms, is raised in energy by shortening $X\cdots X$ contacts. Furthermore, tellurium *p*-block bands are higher in energy than sulfur or selenium *p*-block bands because of the more diffuse nature of the Te *p*-orbitals. Consequently, for a ditelluride MTe_2, the Te *p*-block bands may overlap significantly with the bottom portion of the metal *d*-block bands so that a partial electron transfer occurs from the Te *p*-block bands to the metal *d*-block bands. Given the amount of this electron transfer as ε electrons per metal, the formal oxidation state of the metal in MTe_2 becomes $M^{(4-\varepsilon)+}$ so that the formal *d*-electron count on metal changes accordingly. The structural distortion of a transition-metal compound depends critically on the formal *d*-electron count on the metal (see below). Thus the tellurium-to-metal electron transfer in MTe_2, induced by short Te···Te contacts, could have profound effects upon the structure and electronic properties of MTe_2.

In many layered transition-metal ditellurides MTe_2, short Te···Te contacts occur within each layer as well as between adjacent layers. Thus, in evaluating the extent of the tellurium-to-metal electron transfer, it is also necessary to examine how this electron transfer is affected by the inter- and intralayer Te···Te contacts. In the following, we probe these questions by analyzing the electronic structures of TiX_2 (X = S, Se, Te), MTe_2 (M = V, Nb, Ta), and $IrTe_2$. We calculate the electronic structures of these chalcogenides by employing the extended Hückel tight-binding method (*10*). The atomic parameters used for our calculations are summarized in Table I.

Chalcogen-to-Metal Electron Transfer in TiX_2 (X = S, Se, Te)

As schematically shown in Fig. 1, the structures of CdI_2-type layered transition-metal dichalcogenides TiX_2 (X = S, Se, Te) (*11–13*) are described in terms of TiX_2 layers made up of TiX_6 octahedra. Such TiX_2 layers are stacked together to form three-dimensional (3D) TiX_2 structures. Very often, the interlayer $X\cdots X$ contact interactions are considered to be weak VDW interactions. The inter- and intralayer $X\cdots X$ contacts of TiX_2 shorter than the VDW radii sum (3.6, 3.8, and 4.0 Å for X = S, Se, and Te, respectively) (*14*) are summarized in Table II. With the oxidation state $Ti^{4+}(X^{2-})_2$, a semiconducting property is predicted for all TiX_2 (X = S, Se, Te). This prediction is correct only for TiS_2 (*15*). Both $TiSe_2$ and $TiTe_2$ are metallic, so that their chalcogen *p*-block bands should overlap with the Ti *d*-block bands (*15*).

Figures 2a, 3a, and 4a plot the band dis-

TABLE I

EXPONENTS AND PARAMETERS USED IN THE CALCULATIONS

Atom	Orbital	H_{ii}(eV)	ζ_1	c_1[a]	ζ_2	c_2[a]
Ti	4*s*	−8.90	1.30			
	4*p*	−5.40	1.30			
	3*d*	−11.20	4.55	0.4391	1.60	0.7397
V	4*s*	−8.81	1.30			
	4*p*	−5.52	1.30			
	3*d*	−11.00	4.75	0.4755	1.70	0.7052
Nb	5*s*	−10.10	1.90			
	5*p*	−6.86	1.85			
	4*d*	−12.10	4.08	0.6401	1.64	0.5516
Ta	6*s*	−10.10	2.28			
	6*p*	−6.86	2.24			
	5*d*	−12.10	4.76	0.6597	1.94	0.5589
S	3*s*	−20.00	1.817			
	3*p*	−13.30	1.817			
Se	4*s*	−20.50	2.44			
	4*p*	−13.20	2.07			
Te	5*s*	−20.78	2.51			
	5*p*	−13.20	2.16			

[a] Contraction coefficients used in the double-ζ expansion.

persion relations calculated for 3D TiS_2, $TiSe_2$, and $TiTe_2$, respectively. TiS_2 has a band gap, while $TiSe_2$ and $TiTe_2$ show an expected overlap of their chalcogen *p*-block and Ti *d*-block bands. The results of our calculations are in good agreement with those of other recent studies (*16–18*). The extent of the band overlap is slight in $TiSe_2$ but strong in $TiTe_2$. All these results are consistent with the observed properties of

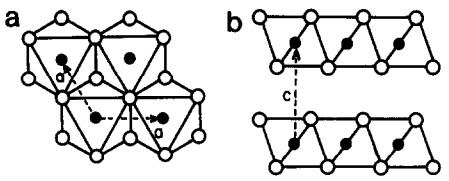

FIG. 1. Structure of a CdI_2-type transition-metal dichalcogenide MX_2. (a) Projection view of a single MX_2 layer along the direction perpendicular to the layer. (b) Cross sectional view perpendicular to the layers. The filled and empty circles represent *M* and *X*, respectively.

TiX_2 (X = S, Se, Te) (*15*). Figures 2b, 3b, and 4b show the total and projected densities of states (DOS) calculated for TiS_2, $TiSe_2$, and $TiTe_2$, respectively. In the case of $TiTe_2$, the Ti *d*-orbital character is significant just below the Fermi level, as expected from the strong band overlap.

According to the Mulliken population analysis (*19*), we calculate the gross atomic populations of Ti in the TiX_2 systems (hereafter denoted by Q_{TiX_2}) summarized in Table II. The *d*-block bands of TiS_2 are empty, so that the Q_{TiS_2} value of 3.760 electrons corresponds to the Ti formal oxidation state d^0 in TiS_2. To a first approximation, the relative value $\Delta Q_X = Q_{TiX_2} - Q_{TiS_2}$ (X = Se, Te) may be regarded as the amount of chalcogen-to-metal electron transfer in TiX_2 (X = Se, Te). From Table II, the values ΔQ_X are calculated to be 0.02 and 0.38 electrons per Ti for $TiSe_2$ and $TiTe_2$, respectively. Namely, the selenium-to-metal electron transfer in $TiSe_2$ is slight, but the tellurium-to-metal electron transfer in $TiTe_2$ is significant.

TABLE II

GROSS ATOMIC POPULATIONS OF METAL ATOMS M; CHALCOGEN CHALCOGEN ($X\cdots X$) CONTACT DISTANCES AND THEIR OVERLAP POPULATIONS IN LAYERED TRANSITION-METAL DICHALCOGENIDES MX_2 (M = Ti, X = S, Se, Te; M = Ir, X = Te).

Compound MX_2	Gross population of M (e^-/atom)	Distance (Å)/Overlap population of $X\cdots X$ (e^-/bond)	
		Interlayer	Intralayer
TiS_2	3.760	3.460/−0.001	3.407[a]/−0.011 3.462[b]/−0.013
$TiSe_2$	3.776	3.548/0.002	3.540[a]/−0.007 3.683[b]/−0.011
$TiTe_2$	4.136	3.775/0.011	3.777[a]/−0.005 4.051[b]/−0.008
$IrTe_2$	9.535	3.498/0.046	3.928[a]/−0.010 3.558[b]/0.010

[a] Within a chalcogen sublayer.
[b] Between chalcogen sublayers.

In general, the overlap population of an $X\cdots X$ contact is negative when all bonding and antibonding levels between two X centers are occupied. This situation arises typically when the formal oxidation state of X is written as X^{2-}. The $X\cdots X$ overlap population can become positive when some electrons are removed from the top portion of the chalcogen p-block bands, which possesses an antibonding character between adjacent X atoms. Consequently, the $X\cdots X$ contacts of TiX_2 primarily responsible for the chalcogen-to-metal electron transfer are those with positive overlap populations. Table II summarizes the overlap populations calculated for the various inter- and intra-

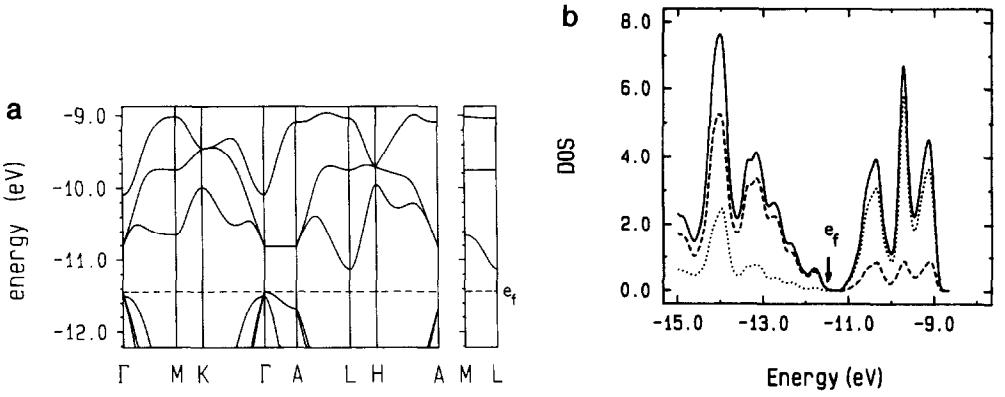

FIG. 2. Calculated band electronic structure of TiS_2. (a) Dispersion relations, where Γ = (0, 0, 0), M = ($\frac{1}{2}$, 0, 0), K = ($\frac{1}{3}$, $\frac{1}{3}$, 0), A = (0, 0, $\frac{1}{2}$), L = ($\frac{1}{2}$, 0, $\frac{1}{2}$), and H = ($\frac{1}{3}$, $\frac{1}{3}$, $\frac{1}{2}$). (b) Total and projected DOS curves. The solid, dotted, and dashed lines refer to the total DOS, the projected DOS for the Ti d orbitals, and the projected DOS for S, respectively.

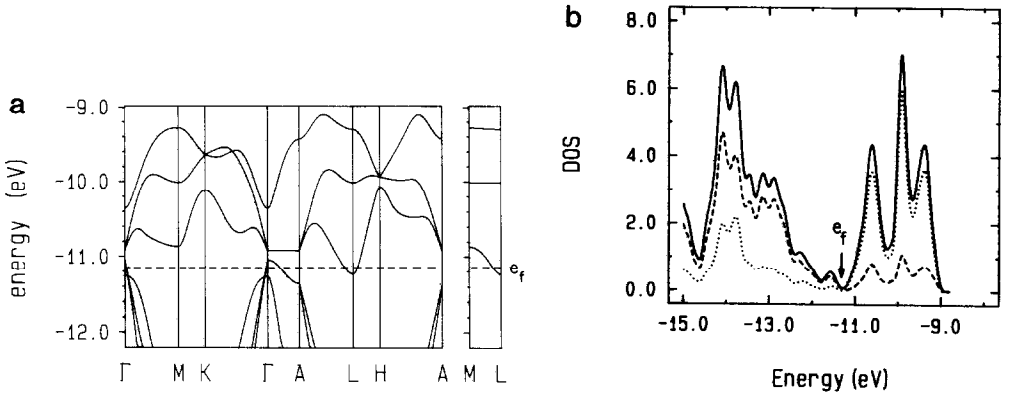

FIG. 3. Calculated band electronic structure of $TiSe_2$. (a) Dispersion relations, where Γ = (0, 0, 0), M = ($\frac{1}{2}$, 0, 0), K = ($\frac{1}{3}$, $\frac{1}{3}$, 0), A = (0, 0, $\frac{1}{2}$), L = ($\frac{1}{2}$, 0, $\frac{1}{2}$), and H = ($\frac{1}{3}$, $\frac{1}{3}$, $\frac{1}{2}$). (b) Total and projected DOS curves. The solid, dotted, and dashed lines refer to the total DOS, the projected DOS for the Ti d orbitals, and the projected DOS for Se, respectively.

layer $X\cdots X$ contacts in TiX_2. It is striking to note that the only $X\cdots X$ contacts with positive overlap populations are the interlayer $X\cdots X$ contacts in $TiSe_2$ and $TiTe_2$, for which there is nonzero chalcogen-to-metal electron transfer. In addition, the overlap population for each interlayer Te···Te contact in $TiTe_2$ is much greater than that for each interlayer Se···Se contact in $TiSe_2$. This is consistent with the finding that the chalcogen-to-metal electron transfer is much greater in $TiTe_2$ than $TiSe_2$.

Distortion and Tellurium-to-Metal Electron Transfer in MTe_2 (M = V, Nb, Ta)

As schematically shown in Fig. 5, layered transition-metal dichalcogenides MX_2 show several interesting distortion patterns of

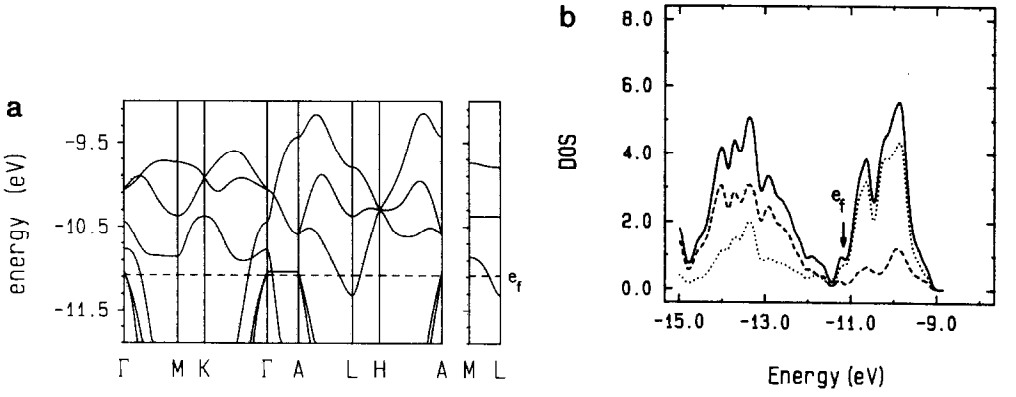

FIG. 4. Calculated band electronic structure of $TiTe_2$. (a) Dispersion relations, where Γ = (0, 0, 0), M = ($\frac{1}{2}$, 0, 0), K = ($\frac{1}{3}$, $\frac{1}{3}$, 0), A = (0, 0, $\frac{1}{2}$), L = ($\frac{1}{2}$, 0, $\frac{1}{2}$), and H = ($\frac{1}{3}$, $\frac{1}{3}$, $\frac{1}{2}$). (b) Total and projected DOS curves. The solid, dotted, and dashed lines refer to the total DOS, the projected DOS for the Ti d orbitals, and the projected DOS for Te, respectively.

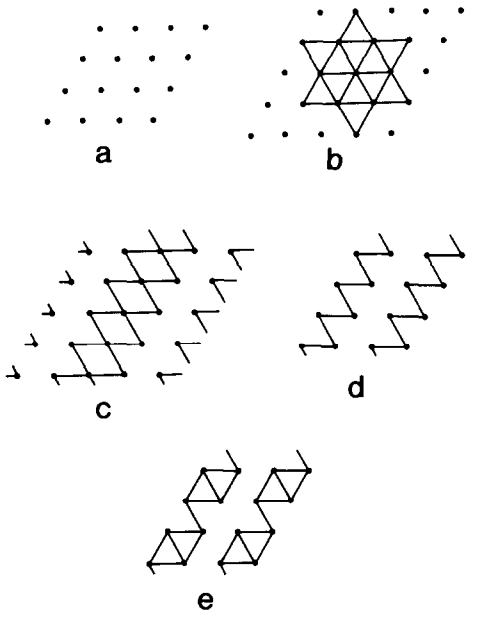

FIG. 5. Distortion patterns in CdI_2-type layered transition-metal dichalcogenides MX_2. Each metal atom is represented by a filled circle. (a) Undistorted hexagonal lattice typically found for d^0 systems; (b) metal atom clustering typically found for d^1 systems; (c) double zigzag chains found for MTe_2 (M = V, Nb, Ta) systems; (d) zigzag chains typically found for d^2 systems; and (e) "diamond" chains typically found for d^3 systems.

metal ions depending upon the formal oxidation state of the metal, or, equivalently, the d-electron count on metal. MX_2 layers with d^0 metal ions show a hexagonal pattern (Fig. 5a), those with d^1 metal ions isolated clusters (Fig. 5b) (*21*), those with d^2 metal ions zigzag chains (Fig. 5d) (*5*, *22*), and those with d^3 metal ions "diamond" chains (Fig. 5e) (*23*). The double zigzag chains of Fig. 5c are found for MTe_2 (M = V, Nb, Ta) (*24*, *25*), and may be considered as a "compromise" of the distortion tendencies toward the clusters of Fig. 5b and the zigzag chains of Fig. 5d. This speculation suggests that the formal d-electron count for MTe_2 (M = V, Nb, Ta) is not d^1 but $d^{1+\varepsilon}$ ($0 < \varepsilon < 1$). This is reasonable because a tellurium-to-metal electron transfer is expected in MTe_2. In the following, we show this to be the case by analyzing the electronic structures of VTe_2 for its undistorted and distorted structures.

VTe_2 has a CdI_2-type structure above 482 K (*24*), which will be referred to as the undistorted structure. Below 482 K, VTe_2 has a distorted structure (*24*), which has double zigzag chains of vanadium ions in each layer and numerous short inter- and intralayer Te···Te contacts. We now examine the effect of the distortion in VTe_2 on the tellurium-to-metal electron transfer. To perform band electronic structure calculations for the undistorted VTe_2 structure, we adopt a V–Te distance of 2.709 Å, the average of the V–Te distances found for the distorted VTe_2 structure. Results of our band electronic structure calculations are summarized in Fig. 6 for the undistorted VTe_2, and in Fig. 7 for the distorted VTe_2. It is clear from the band dispersion relations and the DOS curves of these figures that the overlap between the tellurium p-block and the vanadium d-block bands is significantly enhanced by the distortion.

Table III summarizes our Milliken population analyses for the undistorted and distorted VTe_2 structures. Comparison of the vanadium gross populations for the two structures shows that the distortion leads to a tellurium-to-metal electron transfer of 0.25 electrons per V. There exists no accurate crystal structure of a CdI_2-type VS_2, for which one might assign a formal d^1 electron count for V. Thus, at present, we cannot accurately estimate the amount of tellurium-to-metal electron transfer in the undistorted VTe_2. Nevertheless the formal d-electron count for vanadium in the distorted VTe_2 can be given as $d^{1+\varepsilon}$ with $0.25 < \varepsilon < 1$. This supports our speculation that the distortion toward the double zigzag chains of metal ions in MX_2 is preferred for those MX_2 with a d-electron count between d^1 and d^2.

The Te···Te overlap populations of Table III show that all short interlayer Te···Te

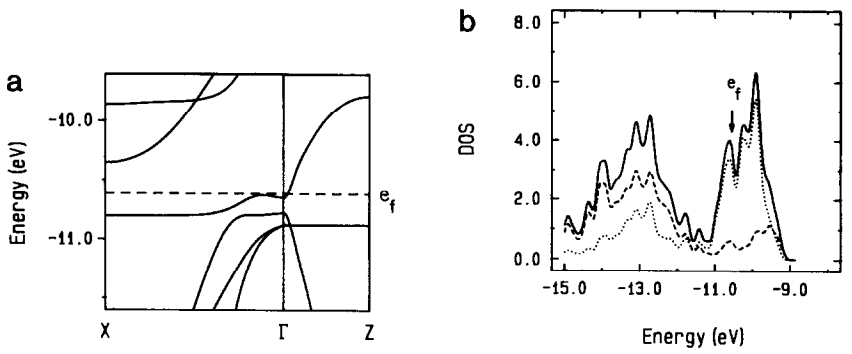

FIG. 6. Calculated band electronic structure of the undistorted VTe_2. (a) Dispersion relations, where $\Gamma = (0, 0, 0)$, $X = (\frac{1}{2}, 0, 0)$, and $Z = (0, 0, \frac{1}{2})$. (b) Total and projected DOS curves. The solid, dotted, and dashed lines refer to the total DOS, the projected DOS for the V *d* orbitals, and the projected DOS for Te, respectively.

contacts of VTe_2 have positive overlap populations, and should therefore be important for the tellurium-to-metal electron transfer. In the distorted VTe_2, two very short intralayer Te···Te contacts also possess positive overlap populations thereby contributing to the electron transfer. It is interesting to observe from Table III that only the shortest V···V contacts making the double zigzag chain paths have positive overlap populations. This supports the description of the distorted VTe_2 in terms of double zigzag chains of vanadium ions.

We also performed band electronic structure calculations for $NbTe_2$ and $TaTe_2$, for which only distorted structures are known (*25*). These calculations show results similar to those obtained for distorted VTe_2.

Discussion

The reference point of the chalcogen-to-metal electron transfer in MX_2 (hereafter referred to as the $p \rightarrow d$ electron transfer) is the oxidation state $M^{4+}(X^{2-})_2$, for which the amount of the $p \rightarrow d$ electron transfer is

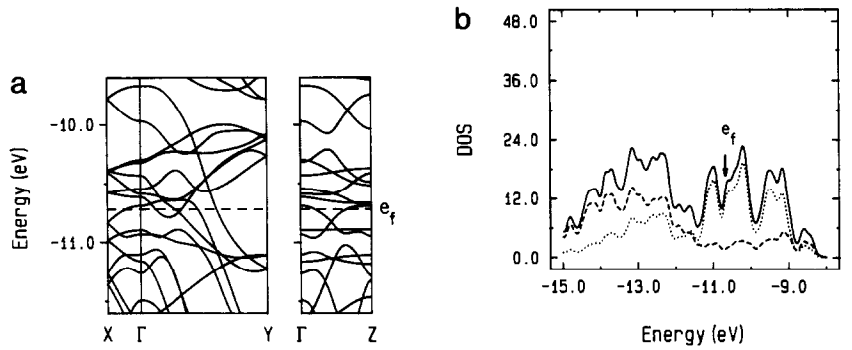

FIG. 7. Calculated band electronic structure of the distorted VTe_2. (a) Dispersion relations, where $\Gamma = (0, 0, 0)$, $X = (\frac{1}{2}, 0, 0)$, $Y = (0, \frac{1}{2}, 0)$, and $Z = (0, 0, \frac{1}{2})$. (b) Total and projected DOS curves. The solid, dotted, and dashed lines refer to the total DOS, the projected DOS for the V *d* orbitals, and the projected DOS for Te, respectively.

TABLE III

GROSS ATOMIC POPULATIONS OF V, V···V AND Te···Te CONTACT DISTANCES, AND THEIR OVERLAP POPULATIONS IN THE UNDISTORTED AND DISTORTED STRUCTURES OF VTe_2

Structure	Gross population of V (e^-/atom)	Distance/Overlap population of V···V (Å) (e^-/bond)	Distance (Å)/Overlap population of Te···Te (e^-/bond)	
			Interlayer	Intralayer
Undistorted	4.986	3.638/−0.009	3.793/0.002	3.638[a]/−0.003
				4.016[b]/−0.007
Distorted	5.234	3.316/0.042	3.590/0.017	3.447[b]/0.014
		3.595/−0.007	3.595/0.009	3.492[a]/0.007
			3.778/0.008	3.738[a]/−0.005
			3.907/0.003	3.742[a]/−0.005
				3.947[b]/−0.008

[a] Within a chalcogen sublayer.
[b] Between chalcogen sublayers.

zero. If an overlap of the chalcogen *p*-block bands with the metal *d*-block bands (hereafter referred to as the *p–d* band overlap) causes a $p \rightarrow d$ electron transfer of ε electrons per metal, then the metal oxidation state becomes $M^{(4-\varepsilon)+}$. The extent of the *p–d* band overlap increases when the metal *d*-block bands are lowered in energy and/or when the chalcogen *p*-block bands are raised in energy. The bottom portion of the *d*-block bands can be lowered by the use of a more electronegative metal atom or by clustering metal atoms. The latter converts nonbonding levels (i.e., the t_{2g}-levels) into metal–metal bonding levels. The top portion of the chalcogen *p*-block bands can be raised by the use of a less electronegative chalcogen atom *X* or by shortening *X*···*X* contact distances. The latter enhances *X*···*X* antibonding interactions, as already mentioned. On the basis of these simple viewpoints, we briefly survey the structures and/or physical properties of layered transition-metal ditellurides in the following.

Experimentally, the *p–d* band overlap is smaller in $HfTe_2$ than in $TiTe_2$ [0.3 (*26*) vs 0.6 (*18*a) eV], and the interlayer Te···Te contacts are longer in $HfTe_2$ than in $TiTe_2$ [3.89 (*27*) vs 3.775 Å]. These findings are consistent with the fact that Hf is less electronegative than Ti, because it leads to a smaller $p \rightarrow d$ electron transfer, and consequently a longer interlayer Te···Te contact for $HfTe_2$. According to this reasoning, $ZrTe_2$, located between two semimetallic compounds $TiTe_2$ and $HfTe_2$, is expected to be also a semimetal instead of a semiconductor (*28*).

In VTe_2, the metal-atom clustering creates lower-lying *d*-block bands while shortening the Te···Te contacts raises the top portion of the Te *p*-block bands. These two factors acting in concert, plus the fact that V is more electronegative than Ti, give rise to a considerably greater *p–d* band overlap in VTe_2 than in $TiTe_2$. However, the amount of the $p \rightarrow d$ electron transfer in VTe_2 should be similar to that in $TiTe_2$, because the formal *d*-electron count of VTe_2 in the absence of the $p \rightarrow d$ electron transfer is already high (i.e., d^1 instead of d^0). Formally, the distortion from the undistorted VTe_2 in Fig. 5a to the distorted VTe_2 in Fig. 5c is a trimerization. It is interesting to observe that the MTe_4 (*M* = Nb, Ta) phases (*29, 30*), for which the metal *d*-electron count is d^1 in the absence of a $p \rightarrow d$ electron transfer as in

MTe_2 (M = V, Nb, Ta), also show a trimerization of metal atoms as well as Te···Te contact shortening.

β-$MoTe_2$ and WTe_2 phases (*22*a) have metal ions with d^2 electron counting in the absence of the $p \rightarrow d$ electron transfer. Although Mo and W are considerably more electronegative than Ti, a band electronic structure study on β-$MoTe_2$ (*5*) indicates that the extent of the $p \rightarrow d$ electron transfer in these compounds cannot be large due to the high d-electron count (i.e., d^2 instead of d^0). In fact, the interlayer Te···Te contacts in β-$MoTe_2$ and WTe_2 do not possess unusually short distances (e.g., the shortest interlayer Te···Te contacts are 3.855 and 3.927 Å for β-$MoTe_2$ and WTe_2, respectively) (*22*a). Thus, the d-electron count for MTe_2 (M = Mo, W) would be $d^{2+\varepsilon}$ with ε close to zero. The formation of "diamond" chains in MX_2 (Fig. 5e) requires a d^3 electron count as in $ReSe_2$ (*23*b) and Mo_2S_3 (*23*d). Formally, the distortion from the zigzag chain of Fig. 5d to the diamond chain of Fig. 5e is a dimerization. Simply speaking, this is related to the fact that each zigzag chain has a $\frac{1}{2}$-filled 1D band. In general, the electronic energy gain by distortion in a 1D chain decreases as the band filling deviates more than $\frac{1}{2}$ (*31*). This may be responsible for why, in β-$MoTe_2$ and WTe_2, a further distortion along the chain direction is not observed.

For ditellurides $IrTe_2$ and $RhTe_2$, the proper oxidation state is given by $M^{3+}(Te^{1.5-})_2$ (M = Ir, Rh) (*6*), for which the d-electron count is d^6. The d-levels of Ir and Rh are low, and so are the t_{2g}-block bands of MTe_2 (M = Ir, Rh). These bands are completely filled by inducing a large amount of $p \rightarrow d$ electron transfer, which is achieved by a strong Te···Te contact shortening (*6*). Table I shows for $IrTe_2$ that the interlayer Te···Te and one of the two Te···Te intralayer bonding contacts are so short that the tellurium framework of $IrTe_2$ and $RhTe_2$ should be regarded as a 3D polymeric network. MTe_2 phases with such a tellurium network occur with metal ions of d-electron count equal to, or greater than, d^6 and are termed polymeric CdI_2-type phases (*6*). The tellurium network polymerization causes a drastic shortening of the c-axis length due to the interlayer Te···Te bonding. When the Te···Te contacts of $TiTe_2$ and $IrTe_2$ and their overlap populations are compared (Table I), it becomes evident that shortening of the interlayer Te···Te contacts are more efficient than shortening of the intralayer Te···Te contacts in enhancing the $p \rightarrow d$ electron transfer.

For polymeric CdI_2-type MTe_2 phases with d-electron count greater than d^6, the e_g-block bands have to be occupied. In general, the e_g-block bands are high in energy because they have a strongly antibonding character for the M–Te bonds. This implies that, to induce a $p \rightarrow d$ electron transfer into the e_g-block bands, the shortening of the Te···Te contacts should be large and hence may induce a lattice strain. One way of lowering the e_g-block levels as well as reducing the tellurium lattice strain in such a case would be to introduce some Te vacancies. Reduction in the metal coordination number from six will create lower-lying d-levels from the e_g-block levels (*20*). In addition, removal of Te atoms from a tight 3D polymeric tellurium network creates lone-pair levels on Te, which are lower-lying in energy than the antibonding levels of short Te···Te contacts. For metal ions with d-electron count greater than d^6, polymeric CdI_2-type might be stabilized by having Te deficiencies.

Concluding Remarks

The present work reveals that, in layered transition-metal ditellurides of the CdI_2-type structure, the interlayer Te···Te contacts are crucial for the $p \rightarrow d$ electron transfer. This is due certainly to the fact that the overlap between the Te p_z orbitals (perpendicular to the layer) associated with the in-

terlayer Te···Te contacts is effective in raising the top portion of the Te *p*-block bands, because the Te atomic orbitals are very diffuse. The interlayer interactions of CdI_2-type MX_2 dichalcogenides are often considered as VDW interactions, which describe interactions between atoms with completely filled valence shells. When the formal chalcogen oxidation state deviates considerably from X^{2-} by a strong $p \rightarrow d$ electron transfer as in $IrTe_2$, the interlayer $X \cdots X$ interactions are no longer VDW interactions.

The Te *p*-block bands mainly involved in the $p \rightarrow d$ electron transfer of CdI_2-type MTe_2 ditellurides are those whose energies are raised primarily by short interlayer Te···Te contacts. Since the p_z orbitals of Te are involved in these bands, the electrons at the Fermi level coming from these bands lead to a metallic character along the interlayer direction. Therefore, the layered ditellurides are expected to possess a 3D metallic character. For the same reason, a slight change in the interlayer Te···Te contact arrangements would have significant effects upon the electrical and other physical properties of these ditellurides. This conclusion is expected to apply equally well to other metallic layered transition-metal tellurides.

Acknowledgments

This work was supported by the U.S. Department of Energy, Office of Basic Sciences, Division of Materials Sciences, under Grant DE-FG05-86ER45259, by NATO, Scientific Affairs Division, and by Centre National de la Recherche Scientifique.

References

1. (a) HULLIGER, F. *in* "Structural Chemistry of Layer-Type Phases" (F. Lévy, Ed.), Reidel, Dordrecht, The Netherlands (1976); (b) P. BÖTTCHER, *Agnew. Chem. Int. Ed. Engl.* **27,** 759 (1988).
2. J. M. WILLIAMS, H. H. WANG, T. J. EMGE, U. GEISER, M. A. BENO, P. C. W. LEUNG, K. D. CARLSON, R. J. THORN, A. J. SCHULTZ, AND M.-H. WHANGBO, *Prog. Inorg. Chem.* **33,** 183 (1985).
3. E. CANADELL, I. E.-I. RACHIDI, J. P. POUGET, P. GRESSIER, A. MEERSCHAUT, J. ROUXEL, D. JUNG, M. EVAIN, AND M.-H. WHANGBO, *Inorg. Chem.* **29,** 1401 (1990).
4. E. CANADELL, Y. MATHEY, AND M.-H. WHANGBO, *J. Am. Chem. Soc.* **110,** 104 (1988).
5. E. CANADELL, AND M.-H. WHANGBO, *Inorg. Chem.* **29,** 1398 (1990).
6. S. JOBIC, P. DENIARD, R. BREC, J. ROUXEL, A. JOUANNEAUX, AND A. N. FITCH, *Z. Anorg. Allg. Chem.* **598/599,** 199 (1991).
7. S. JOBIC, M. EVAIN, R. BREC, P. DENIARD, A. JOUANNEAUX, AND J. ROUXEL, submitted for publication.
8. S. JOBIC, R. BREC, AND J. ROUXEL, *J. Solid State Chem.* **96,** 169 (1992).
9. E. CANADELL, S. JOBIC, R. BREC, AND J. ROUXEL, in press.
10. (a) M.-H. WHANGBO AND R. HOFFMANN, *J. Am. Chem. Soc.* **100,** 6093 (1978); (b) M.-H. WHANGBO, R. HOFFMANN, AND R. B. WOODWARD, *Proc. R. Soc. London Ser. A* **366,** 23 (1979).
11. For the crystal structure of TiS_2 employed in our calculations, see: C. RIEKEL AND R. SCHÖLLHORN, *Mater. Res. Bull.* **10,** 629 (1975).
12. For the crystal structure of $TiSe_2$ employed in our calculations, see: C. RIEKEL, *J. Solid State Chem.* **17,** 389 (1976).
13. For the crystal structure of $TiTe_2$ employed in our calculations, see: C. RIEKEL, M. THOMAS, AND R. SCHÖLLHORN, *Phys. Status Solidi (A)* **50,** K231 (1978).
14. A. BONDI, *J. Phys. Chem.* **68,** 441 (1964).
15. For a recent review on the physical properties and band electronic structures of TiX_2 (X = S, Se, Te), see: E. DONI AND R. GIRLANDA, *in* "Electronic Structure and Electronic Transitions in Layered Materials" (V. Grasso, Ed.), p. 1, Reidel, Dordrecht, The Netherlands (1986).
16. For recent band electronic structure calculations on TiS_2, see: (*a*) A. ZUNGER AND A. J. FREEMAN, *Phys. Rev. B* **16,** 906 (1977); (b) D. W. BULLETT, *J. Phys. C* **11,** 4501 (1978); (c) J. VON BOEHM AND H. M. ISOMÄKI, *J. Phys. C* **15,** L733 (1982); (d) C. UMRIGAR, D. E. ELLIS, D. S. WANG, H. KRAKAUER, AND M. POSTERNAK, *Phys. Rev. B* **26,** 4935 (1982); (f) N. SUZUKI, T. YAMASAKI, AND K. MOTIZUKI, *J. Phys. C* **21,** 6133 (1988).
17. For recent band electronic structure calculations on $TiSe_2$, see: (a) H. M. MYRON AND A. J. FREEMAN, *Phys. Rev. B* **9,** 481 (1974); (b) A. ZUNGER AND A. J. FREEMAN, *Phys. Rev. B* **17,** 1839 (1978); (c) Ref. (*16*b); (d) H. ISOMÄKI, J. VON BOEHM, AND P. KRUSIUS, *J. Phys. C* **12,** 3239 (1979); (e) J. VON BOEHM, AND H. M. ISOMÄKI, *J. Phys. C* **14,** L75 (1981).

18. For recent band electronic structure calculations on $TiTe_2$, see: (a) D. K. G. DE BOER, C. F. VAN BRUGGEN, G. W. BUS, R. COEHOORN, G. A. SAWATZKY, H. W. MYRON, D. NORMAN, AND H. PADMORE, *Phys. Rev. B* **29,** 6797 (1984); (b) Ref. (*16*b).
19. R. S. MULLIKEN, *J. Chem. Phys.* **23,** 1833, 1841, 2338, 2343 (1955).
20. T. A. ALBRIGHT, J. K. BURDETT, AND M.-H. WHANGBO, "Orbital Interactions in Chemistry," Wiley, New York (1985).
21. (a) R. BROUWER AND F. JELLINEK, *Physica B* **99,** 51 (1980); (b) J. A. WILSON, F. J. DISALVO, AND S. MAHAJAN, *Adv. Phys.* **24,** 117 (1975).
22. (a) B. E. BROWN, *Acta Crystallogr.* **20,** 268 (1966); (b) S. MEERSCHAUT, M. SPIESSER, J. ROUXEL, AND O. GOROCHOV, *J. Solid State Chem.* **31,** 31 (1980).
23. (a) E. CANADELL, A. LEBEUZE, M. A. EL KHALIFA, R. CHEVREL, AND M.-H. WHANGBO, *J. Am. Chem. Soc.* **111,** 3778 (1989); (b) N. W. ALCOCK AND A. KJEKSHUS, *Acta Chem. Scand.* **19,** 79 (1965); (c) J. C. WILDERVANCK, AND F. JELLINEK, *J. Less-Common Met.* **24,** 73 (1971); (d) R. DEBLIEK, G. A. WIEGERS, K. D. BRONSEMA, D. VAN DYCK, G. VAN TENDELOO, J. VAN LANDUYT, AND S. AMELINCKX, *Phys. Status Solidi A* **77,** 249 (1983).
24. K. D. BRONSEMA, G. W. BUS, AND G. A. WIEGERS, *J. Solid State Chem.* **53,** 415 (1984).
25. B. E. BROWN, *Acta Crystallogr.* **20,** 264 (1966).
26. P. C. KLIPSTEIN, D. R. P. GUY, E. A. MARSEGLIA, J. I. MEAKIN, R. H. FRIEND, AND A. D. YOFFE, *J. Phys. C* **19,** 4953 (1986).
27. Since only the cell parameters are known for $HfTe_2$, the z-value of $TiTe_2$ was used to calculate the Te···Te contact distances of $HfTe_2$.
28. Some band electronic structure calculations predict $ZrTe_2$ to be a semiconductor. For example, see Ref. (*16*b).
29. (a) S. VAN SMAALEN, K. D. BRONSEMA, AND J. MAHY, *Acta Crystallogr. Sect. B.* **42,** 43 (1986); (b) K. SELTE AND A. KJEKSHUS, *Acta Chem. Scand.* **18,** 690 (1964); (c) F. W. BOSWELL, A. PRODAN, AND J. BRANDON, *J. Phys. C* **16,** 1067 (1983); (d) H. BÖHM AND H. G. VON SCHNERING, *Z. Kristallogr.* **162,** 26 (1983); (e) H. BÖHM *Z. Kristallogr.* **180,** 113 (1987).
30. (a) K. D. BRONSEMA, S. VAN SMAALEN, J. L. DE BOER, AND J. MAHY, *Acta Crystallogr. Sect. B.* **43,** 305 (1987); (b) E. BJERKELUND AND A. KJEKSHUS, *J. Less-Common Met.* **7,** 231 (1964).
31. M.-H. WHANGBO, "Crystal Structures and Properties of Materials with Quasi-One-Dimensional Structures" (J. Rouxel, Ed.), p. 27, Reidel, Dordrecht, The Netherlands, (1986).